Crystal Structure of Methotrexate Tetrahydrate

Paul A. Sutton, Vivian Cody,* and G. David Smith

Contribution from the Medical Foundation of Buffalo, Inc., Buffalo, New York 14203.
Received November 29, 1985

Abstract: The single-crystal structure of methotrexate (MTX), a diaminofolic acid analogue, has been determined to elucidate its conformational and electronic properties. Crystals of MTX·4H_2O are tetragonal, space group $P4_12_12$ with unit cell dimensions a = 10.372 (1) and c = 45.546 (7) Å, Z = 8, and V = 4899.7 (2) Å^3. The agreement index is 0.078 for 2240 unique data with $I > 3\sigma(I)$. The molecular conformation of MTX differs from that observed for the enzyme-bound inhibitor. The largest differences involve a cis/trans orientation about the torsion angle N(5)–C(6)–C(9)–N(10) between the pteridine ring and the (*p*-aminobenzoyl)glutamate and a gauche conformation for the glutamate. The γ-carboxylate is disordered (80:20) by a 74° rotation about the C(21)–C(22) bond. In addition water-3 is disordered with occupancies of 40:40:20. There are no N···N hydrogen bonds in the crystal structure, as observed in other antifolate structures. There is a remarkable agreement in pteridine ring hydrogen bonding between the title compound and MTX bound to the enzyme active site. The packing shows that the α-carboxylate oxygens form hydrogen bonds to N(1) and N(2), the major γ-carboxylate conformer forms hydrogen bonds to N(2) and N(4), the carbonyl oxygen of the peptide forms a hydrogen bond to N(4), and a water molecule makes a short intermolecular contact to N(8). In addition, MTX is protonated at N(1). These data show that the intermolecular contacts observed in this structure are relevant to those found in the enzyme active-site environment and also provide reliable details of the hydrogen-bond strengths and directionality.

Dihydrofolate reductase (DHFR), a necessary component of mammalian cells, catalyzes the reduction of dihydrofolate to tetrahydrofolate and plays an essential role in maintaining levels of tetrahydrofolate coenzymes in cells. Diaminopteridine analogues of folic acid have been shown to inhibit DHFR and ultimately deprive cells of requisite substrates for DNA replication, which subsequently led to their use as chemotherapeutic agents for infectious and neoplastic diseases.[1-3] Methotrexate (MTX), a diaminofolic acid analogue, is the most widely used antifolate chemotherapeutic agent. Replacement of the folic acid 4-carbonyl oxygen by an amine and methylation of N(10) produce large changes in its chemical properties and binding affinity to DHFR. These changes are reflected in the increased basicity and ease of protonation of the diaminopteridine ring in MTX. The N(1) dissociation constant (pK_a) for folic acid is 2.35 and 5.71 for MTX. The pK_a of the α-carboxylate is 3.36 in MTX but could not be measured for folic acid.[4] Binding affinity data also show that MTX is more tightly bound to DHFR when protonated at N(1), whereas folic acid binds best as a neutral species.[3] The crystal structure of MTX has been determined to elucidate its conformational and electronic properties.

Crystallographic data delineating the DHFR enzyme structure and inhibitor/cofactor complexes are available from two bacterial and one avian species.[5,6] These data demonstrate that the active site is lined by hydrophobic side chains and show that MTX binds to the enzyme with the pteridine ring nearly perpendicular to the benzoyl ring. Data from the 1.7-Å refinement of both bacterial DHFR enzyme structures show that Asp-26 (*Lactobacillus casei* numbering) forms strong hydrogen bonds to N(1) and N(2); a water molecule hydrogen bonds to N(2) and N(8), and the hydrogens of N(4) are involved in hydrogen bonds with the carbonyl oxygens of Ala-97 and Leu-4.[5] Furthermore, NMR evidence indicates that MTX is protonated at N(1) in the enzyme active site.[7]

The crystal structure of MTX is useful for computer graphic modeling studies with the enzyme active site and for parameterization of molecular mechanics programs, as both processes are important for computer-aided drug design. Analysis of hydrogen bonding and molecular packing of crystalline MTX offers insight into the molecular details of hydrogen-bond strength and directionality of drug binding to the enzyme active site. The similarities in hydrogen bonding between both crystalline and enzyme bound forms of MTX support the importance of this structure for future binding studies.

Experimental Section

Methotrexate crystals were found to grow from a water and ethanol (10:1 v/v) mixture at a pH between 3.5 and 4.5. The pH was adjusted with NaH_2PO_4 and H_3PO_4. Crystals of MTX·4H_2O are tetragonal, space group $P4_12_12$ or its enantiomorph $P4_32_12$, with unit cell dimensions a = 10.372 (1) Å, c = 45.546 (7) Å, Z = 8, V = 4899.7 (2) Å^3. The crystal used for data collection was rectangular with dimensions 0.20 × 0.30 × 0.44 mm. Data were collected on a Nonius CAD-4 diffractometer with Cu Kα radiation. A total of 2787 unique reflections was collected to 2θ = 130°. The structure was solved with the direct methods programs MULTAN[8] and NQEST.[9] All heavy atoms, except water-4, were refined anisotropically by full-matrix least-squares techniques. Since water-4 lies on a twofold axis, only x and B_{iso} were refined. The γ-carboxylate and water-3 were disordered; their occupancies were 80:20 and 40:40:20, respectively. Disorder of C(22) was investigated since it had a higher than expected thermal parameter; however, no disorder could be resolved. Hydrogen atoms were placed in calculated positions and given isotropic thermal parameters 1 unit greater than the heavy atoms to which they were bound. Final positional and isotropic thermal parameters for heavy atoms are listed in Table I. The final R value was 0.078 for 2240 data with $I > 3\sigma(I)$.

Results and Discussion

The molecular conformation of MTX is folded with a 97° angle between the plane of the pteridine ring and *p*-aminobenzoyl ring (Figure 1). The glutamate moiety is also folded and shows disorder of the γ-carboxylate position. The disorder results from a 74° rotation of the carbon adjacent to the γ-carboxylate.

As illustrated in Figure 2, the molecular conformation of MTX differs significantly from that observed for the enzyme-bound inhibitor. Table II shows the numbering scheme of MTX and lists major conformational differences among related structures. The major differences involve rotations about the bonds C(6)–C(9), C(14)–C(17), N(18)–C(19), and C(21)–C(22). The net effect of these differences in the MTX structure is to have the

(1) Bertino, J. R.; McGuire, J. J. In *Chemistry and Biology of Pteridines*; Blair, J. A., Ed.; Walter de Gruyter: New York, 1983; pp 263-274.
(2) Blakley, R. L.; Benkovic, S. J. *Folates and Pterins*; Wiley: New York, 1984; Vol. 1.
(3) Roth, B.; Bliss, E.; Beddell, C. R. In *Molecular Aspects of Anticancer Drug Action*; Neidle, S., Waring, M. J., Eds.; Verlag Chemie: Basel, 1983; pp 363-393.
(4) Poe, M. *J. Biol. Chem.* **1977**, *252*, 3724-3729.
(5) Bolin, J. T.; Filman, D. J.; Matthews, D. A.; Hamlin, R. C.; Kraut, J. *J. Biol. Chem.* **1982**, *257*, 13650-13662.
(6) Matthews, D. A.; Bolin, J. T.; Burridge, J. M.; Filman, D. J.; Volz, K. W.; Kaufman, B. T.; Beddell, C. R.; Champness, J. N.; Stammers, D. K.; Kraut, J. *J. Biol. Chem.* **1985**, *260*, 381-391.
(7) Blakley, R. L. In *Folates and Pterins*; Blakley, R. L., Benkovic, S. J., Eds.; Wiley: New York, 1984; Vol. 1, pp 191-253.
(8) Germain, G.; Main, P.; Woolfson, M. M. *Acta Crystallogr., Sect. A* **1971**, *27*, 368-376.
(9) De Titta, G. T.; Edmonds, J. W.; Langs, D. A.; Hauptman, H. A. *Acta Crystallogr., Sect. A* **1975**, *31*, 472-479.

0002-7863/86/1508-4155$01.50/0

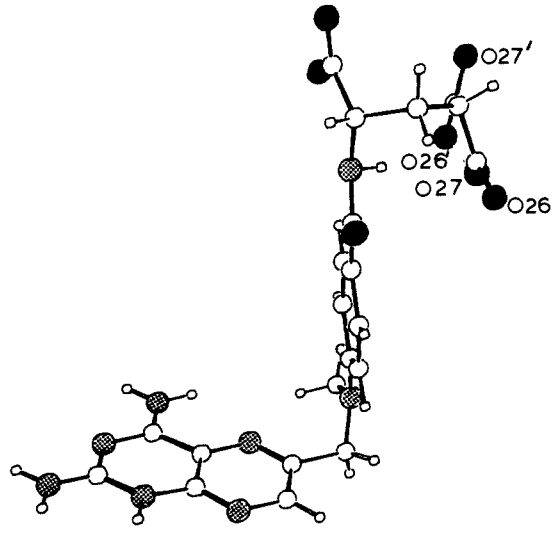

Figure 1. Molecular conformation of methotrexate showing disordered γ-carboxylate. Atoms C(23), O(26) and O(27) have 80% occupancy, and C(23'), O(26') and O(27') have 20% occupancy. The oxygens are filled circles, and nitrogens are stippled.

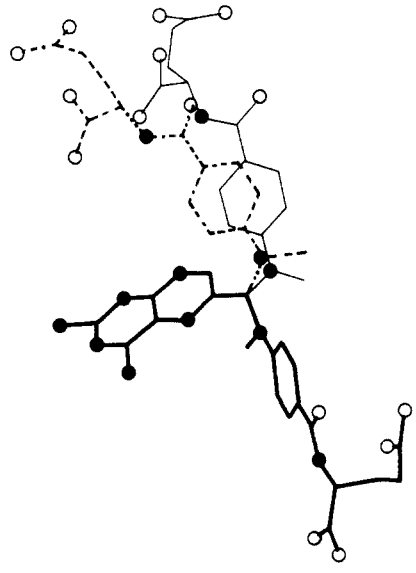

Figure 2. Conformational comparison of MTX: this study (heavy line); *L. casei* (dashed line); *Escherichia coli*, molecule A (light line).

(*p*-aminobenzoyl)glutamate side chain oriented on the opposite side of the pteridine plane compared with MTX observed in the enzyme (Figure 2). MTX also differs from the extended conformation reported for folic acid,[10,11] 5,10-methylenetetrahydrofolate,[12] and quinazoline.[13] [Another MTX conformation, with a different C(6)–C(9) orientation, was reported by Mastropaolo et al. American Crystallographic Association, Stanford, CA, 1985.]

As shown in Table III, the C(22)–C(23') and C(23')–O(27') bond lengths in the minor γ-carboxylate conformer are unusually short. In addition, the differences between the C–O distances in the α- and γ-carboxylates suggest that the α-carboxylate is anionic, while the two disordered γ-carboxylate conformers are protonated.

The average bond length of the eight C–N endocyclic bonds in the pteridine ring of MTX is 1.34 (2) Å, while the average bond length of the two exocyclic C–N bonds is 1.29 (2) Å, suggesting pronounced double-bond character in the amino groups. These results are also consistent with similar values [1.34 (2) and 1.31 (1) Å, respectively] reported for 2,4-diaminopteridines protonated at N(1). The differences between endocyclic and exocyclic C–N bond lengths diminish in nonprotonated pteridine structures.[14]

(10) Mastropaolo, D.; Camerman, A.; Camerman, N. *Science (Washington, D.C.)* **1980**, *210*, 334–336.
(11) Camerman, A.; Mastropaolo, D.; Camerman, N. In *Molecular Structure and Biological Activity*; Griffin, J. F., Duax, W. L., Eds.; Elsevier Biochemical: New York, 1982; pp 1–12.
(12) Fontecilla-Camps, J. C.; Bugg, C. E.; Temple, C., Jr.; Rose, J. D.; Montgomery, J. A.; Kisliuk, R. I. *J. Am. Chem. Soc.* **1979**, *101*, 6114–6115.
(13) Mastropaolo, D.; Smith, H. W.; Camerman, A.; Camerman, N. *J. Med. Chem.* **1986**, *29*, 155–158.

Table I. Atomic Coordinates (×10⁴) and Isotropic Thermal Parameters (×10) for Methotrexate Tetrahydrate

	X/a (σ)	Y/b (σ)	Z/c (σ)	B_{iso},[a] Å²
C(2)	3688 (6)	5399 (6)	7999 (1)	51 (2)
C(4)	4735 (6)	5433 (6)	8445 (1)	49 (2)
C(4A)	5573 (6)	4379 (6)	8356 (1)	46 (1)
C(6)	7185 (6)	2953 (6)	8433 (1)	50 (2)
C(7)	7029 (7)	2516 (6)	8149 (1)	59 (2)
C(8A)	5387 (6)	3888 (6)	8075 (1)	51 (2)
C(9)	8207 (7)	2376 (7)	8635 (1)	59 (2)
C(10)	7994 (8)	3236 (7)	9141 (1)	67 (2)
C(11)	6738 (6)	1360 (6)	8983 (1)	46 (1)
C(12)	6075 (6)	1346 (6)	9251 (1)	54 (2)
C(13)	5096 (6)	479 (6)	9306 (1)	53 (2)
C(14)	4721 (6)	−428 (6)	9098 (1)	46 (1)
C(15)	5392 (6)	−417 (6)	8836 (1)	52 (2)
C(16)	6379 (7)	431 (6)	8778 (1)	53 (2)
C(17)	3685 (6)	−1378 (6)	9143 (1)	49 (2)
C(19)	2147 (7)	−2429 (6)	9477 (1)	58 (2)
C(20)	1391 (7)	−2018 (8)	9746 (1)	60 (2)
C(21)	2722 (8)	−3772 (7)	9509 (2)	69 (2)
C(22)	3780 (12)	−3817 (9)	9730 (2)	106 (4)
C(23)	5040 (12)	−3418 (10)	9622 (2)	73 (3)
C(23')	4223 (43)	−3108 (38)	9921 (7)	62 (11)
N(1)	4432 (6)	4384 (5)	7905 (1)	57 (1)
N(2)	2806 (5)	5833 (5)	7828 (1)	62 (2)
N(3)	3850 (5)	5917 (5)	8266 (1)	51 (1)
N(4)	4853 (6)	5896 (5)	8710 (1)	63 (2)
N(5)	6473 (5)	3894 (5)	8538 (1)	51 (1)
N(8)	6110 (6)	2944 (5)	7969 (1)	60 (2)
N(10)	7756 (5)	2193 (5)	8933 (1)	53 (1)
N(18)	3135 (5)	−1453 (5)	9408 (1)	52 (1)
O(17)	3314 (4)	−2095 (4)	8941 (1)	57 (1)
O(24)	1754 (5)	−1058 (5)	9887 (1)	72 (1)
O(25)	438 (5)	−2669 (6)	9804 (1)	87 (2)
O(26)	5371 (7)	−3967 (8)	9375 (2)	94 (3)
O(26')	5028 (34)	−2078 (30)	9946 (7)	94 (11)
O(27)	5727 (8)	−2683 (8)	9747 (2)	88 (3)
O(27')	3768 (29)	−3586 (31)	10114 (6)	94 (10)
O(W1)	8372 (7)	2472 (9)	1654 (1)	125 (3)
O(W2)	967 (8)	5603 (13)	2527 (1)	216 (6)
O(W3)	9303 (49)	3418 (44)	2162 (13)	172 (16)
O(W3')	9504 (24)	4491 (28)	1958 (5)	82 (8)
O(W3'')	9692 (65)	3934 (44)	2149 (17)	167 (16)
O(W4)	1672 (22)	8328	2500	239 (5)

[a] $B_{iso} = {}^4/_3\sum_i\sum_j\beta_{ij}(a_i a_j)$.

Table II. Conformational Comparison (deg) of MTX

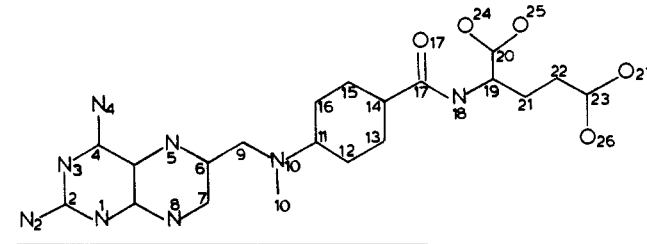

angle	MTX	*L. casei*[a]	*E. coli* A[a]	*E. coli* B[a]
N(5)–C(6)–C(9)–N(10)	39	−168	178	−156
C(6)–C(9)–N(10)–C(11)	63	63	75	58
C(13)–C(14)–C(17)–N(18)	7	97	157	148
C(14)–C(17)–N(18)–C(19)	−177	180	−179	−176
C(17)–N(18)–C(19)–C(21)	79	−175	109	100
N(18)–C(19)–C(21)–C(22)	56	179	−145	−180
C(19)–C(21)–C(22)–C(23)	−83 (11)[b]	−158	127	−152

[a] Coordinates for MTX were obtained from the Brookhaven Protein Data Bank.[5] [b] Involving C(23').

Table III. Bond Distances and Bond Angles for Methotrexate

	Bond Lengths, Å		
C(2)–N(1)	1.372 (8)	C(12)–C(13)	1.379 (9)
C(2)–N(2)	1.281 (8)	C(13)–C(14)	1.391 (8)
C(2)–N(3)	1.341 (7)	C(14)–C(15)	1.381 (8)
C(4)–C(4A)	1.454 (8)	C(14)–C(17)	1.473 (8)
C(4)–N(3)	1.326 (8)	C(15)–C(16)	1.375 (9)
C(4)–N(4)	1.305 (7)	C(17)–N(18)	1.338 (7)
C(4A)–C(8A)	1.392 (8)	C(17)–O(17)	1.244 (7)
C(4A)–N(5)	1.347 (7)	C(19)–C(20)	1.514 (9)
C(6)–C(7)	1.379 (8)	C(19)–C(21)	1.522 (10)
C(6)–C(9)	1.525 (9)	C(19)–N(18)	1.475 (8)
C(6)–N(5)	1.315 (8)	C(20)–O(24)	1.243 (9)
C(7)–N(8)	1.333 (9)	C(20)–O(25)	1.226 (10)
C(8A)–N(1)	1.356 (8)	C(21)–C(22)	1.491 (14)
C(8A)–N(8)	1.324 (8)	C(22)–C(23)	1.457 (17)
C(9)–N(10)	1.449 (8)	C(22)–C(23′)	1.227 (37)
C(10)–N(10)	1.459 (9)	C(23)–O(26)	1.307 (13)
C(11)–C(12)	1.401 (8)	C(23′)–O(26′)	1.361 (53)
C(11)–C(16)	1.393 (8)	C(23)–O(27)	1.189 (14)
C(11)–N(10)	1.382 (8)	C(23′)–O(27′)	1.116 (45)
	Bond Angles, deg		
N(1)–C(2)–N(2)	118.9 (4)	C(14)–C(17)–N(18)	118.4 (4)
N(1)–C(2)–N(3)	121.2 (4)	C(14)–C(17)–O(17)	121.5 (4)
N(2)–C(2)–N(3)	119.9 (4)	N(18)–C(17)–O(17)	120.0 (4)
C(4A)–C(4)–N(3)	121.8 (4)	C(20)–C(19)–C(21)	112.5 (5)
C(4A)–C(4)–N(4)	118.6 (4)	C(20)–C(19)–N(18)	109.8 (5)
N(3)–C(4)–N(4)	119.6 (4)	C(21)–C(19)–N(18)	112.1 (5)
C(4)–C(4A)–C(8A)	116.6 (4)	C(19)–C(20)–O(24)	119.1 (5)
C(4)–C(4A)–N(5)	121.6 (4)	C(19)–C(20)–O(25)	116.0 (5)
C(8A)–C(4A)–N(5)	121.8 (4)	O(24)–C(20)–O(25)	124.9 (5)
C(7)–C(6)–C(6)	121.2 (5)	C(19)–C(21)–C(22)	112.4 (6)
C(7)–C(6)–N(5)	121.3 (4)	C(21)–C(22)–C(23)	115.0 (8)
C(9)–C(6)–N(5)	117.5 (4)	C(21)–C(22)–C(23′)	137.3 (16)
C(6)–C(7)–N(8)	123.5 (5)	C(23)–C(22)–C(23′)	74.5 (15)
C(4A)–C(8A)–N(1)	119.0 (4)	C(22)–C(23)–O(26)	113.8 (8)
C(4A)–C(8A)–N(8)	121.8 (4)	C(22)–C(23)–O(27)	123.9 (8)
N(1)–C(8A)–N(8)	119.2 (4)	O(26)–C(23)–O(27)	122.3 (8)
C(6)–C(9)–N(10)	113.1 (5)	C(22)–C(23′)–O(27′)	97.7 (22)
C(12)–C(11)–C(16)	116.4 (4)	C(22)–C(23′)–O(26′)	139.5 (26)
C(12)–C(11)–N(10)	121.7 (4)	O(27′)–C(23′)–O(26′)	122.8 (27)
C(16)–C(11)–N(10)	121.7 (4)	C(2)–N(1)–C(8A)	121.8 (4)
C(11)–C(12)–C(13)	121.8 (5)	C(2)–N(3)–C(4)	119.5 (4)
C(12)–C(13)–C(14)	121.5 (5)	C(4A)–N(5)–C(6)	116.2 (4)
C(13)–C(14)–C(15)	116.3 (4)	C(7)–N(8)–C(8A)	115.3 (4)
C(13)–C(14)–C(17)	124.2 (4)	C(9)–N(10)–C(10)	117.1 (4)
C(15)–C(14)–C(17)	119.6 (4)	C(9)–N(10)–C(11)	118.9 (4)
C(14)–C(15)–C(16)	123.1 (4)	C(10)–N(10)–C(11)	119.0 (4)
C(11)–C(16)–C(15)	120.9 (5)	C(17)–N(18)–C(19)	121.9 (4)

These data are consistent with protonation at N(1) by the α-carboxylic acid in the MTX crystal structure.

The pteridine ring with substituents N(2) and N(4) is planar to within 0.024 Å, and the *p*-aminobenzoyl ring with substituent C(17) is planar to within 0.007 Å. The substituent atom C(9) is less than 0.047 Å from the least-squares plane of the pteridine ring, and atom N(10) is 0.046 Å out of the plane of the *p*-aminobenzoyl group.

Crystallization of MTX near pH 4 favors protonation at N(1) and ionization of the α-carboxylate since these groups have measured pK_a values of 5.71 and 3.36, respectively.[4] These data are consistent with zwitterion formation suggested by the geometry and hydrogen bonding observed in this structure.

Crystal Packing and Hydrogen Bonding

A characteristic feature observed in the crystal structures of other antifolates is the preferential formation of pseudo base pair N···N hydrogen bonds between adjacent molecules in the crystal packing.[14,15] However, as demonstrated by the data in Table IV and Figure 3, the hydrogen bonding involving the diaminopteridine ring of MTX has no N···N hydrogen bonds and is, furthermore, remarkably similar to that observed for the enzyme-bound

(14) Schwalbe, C. H.; Cody, V. In *Chemistry and Biology of Pteridines*; Blair, J. A., Ed.; Walter de Gruyter: New York, 1983; 511–515.
(15) Cody, V.; Zakrzewski, S. F. *J. Med. Chem.* **1982**, *25*, 427–430.

Table IV. Intermolecular Contacts Less than 3.2 Å

D···A	dist, Å	D···A	dist, Å
N(1)···O(24)	2.690 (7)	O(26)···O(W1)	2.479 (10)
N(2)···O(25)	2.772 (7)	O(27)···O(W3)	2.92 (6)
N(2)···O(27)	2.906 (10)	O(27′)···O(W3)	3.06 (6)
N(3)···O(W1)	2.943 (10)	O(26′)···O(W2)	2.968 (34)
N(4)···O(17)	2.828 (7)	O(26′)···O(W3)	1.99 (7)
N(4)···O(26)	3.081 (9)	O(26′)···O(W3″)	2.14 (8)
N(8)···O(W2)	3.096 (12)	O(W1)···O(W3′)	2.77 (3)
O(17)···O(W1)	2.888 (8)	O(W1)···O(W3)	2.69 (6)
O(24)···O(W2)	2.951 (12)	O(W1)···O(W3″)	3.04 (7)
O(25)···O(W3′)	2.66 (3)	O(W2)···O(W4)	2.92 (2)
O(25)···O(W3)	2.77 (6)	O(W2)···O(W4)	2.92 (2)
O(25)···O(W3″)	2.71 (6)	O(W2)···O(W3″)	2.78 (7)

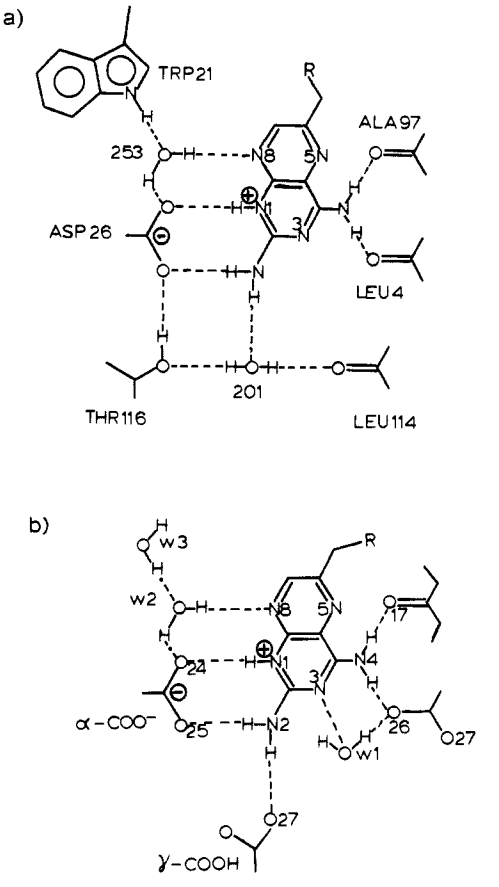

Figure 3. (a) Schematic representation of the hydrogen bonding between DHFR and the pteridine portion of MTX.[2] The numbering scheme of *L. casei* is used. (b) Schematic representation of the hydrogen bonding of MTX·4H_2O in the crystal structure. Note the remarkable similarity in their hydrogen bonding details.

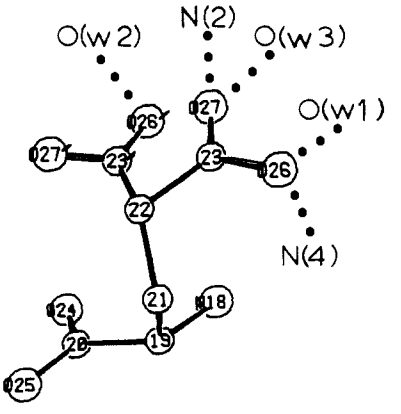

Figure 4. Conformation of the glutamate moiety and schematic representation of the intermolecular contacts with the disordered γ-carboxylate.

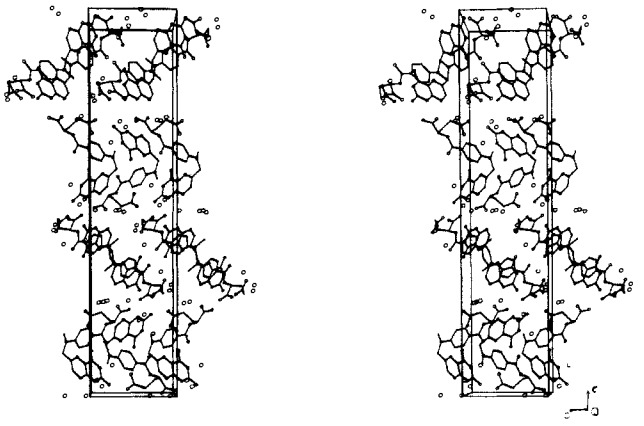

Figure 5. Stereodiagram illustrating molecular packing of MTX·$4H_2O$.

structure (Figure 3a). As noted for the enzyme-bound MTX, these data (Figure 3b) show that strong hydrogen bonds are formed between the α-carboxylate oxygens with N(1) and N(2); in addition, N(2) forms a second hydrogen bond with an oxygen from the γ-carboxylate. Similarly, N(4) forms weaker hydrogen bonds to the carbonyl oxygens O(17) and O(26). There is also a short intermolecular contact between N(8) and a water molecule, as observed in the enzyme structure.

The conformation of the glutamate moiety and a schematic of the intermolecular contacts for the disordered γ-carboxylate are illustrated in Figure 4. There are four intermolecular hydrogen-bonding contacts to the major conformer [O(26), O(27)] and only one to the minor conformer [O(26'), O(27')] (Table IV). However, two of the contacts to the major conformer have poor hydrogen-bonding geometries; the angles N(2)–H(2)···O(27) and N(4)–H(4)···O(26) are 141.6 and 119.5°, respectively. In addition to the disordered γ-carboxylate, water-3 has at least three possible positions (Table I). Thus, the O(27)···O(W3) contact is only partially occupied. The short contacts of O(W3) and O(W3'') with O(26') suggest that only O(W3') exists in concert with the minor γ-carboxylate conformer. Water-3 maintains similar contacts to O(25) and O(W1) among its three positions. Since O(W4) lies on a twofold axis, it has two identical contacts with O(W2). One possible intramolecular hydrogen bond exists between N(18) and O(24) with a distance of 2.640 Å.

As shown in the stereopacking diagram (Figure 5), the fourfold symmetry of this crystal structure permits the MTX molecules to pack in such a manner that the α-carboxylate is in a favorable position to hydrogen bond to the pteridine ring, as observed in the bound enzyme. Also, hydration occurs in clusters along channels between the MTX molecules across the fourfold axis.

The conformational differences observed in MTX structures suggest that it has considerable flexibility, particularly with respect to rotations about the C(6)–C(9) bond. The observation that the specific interactions of the pteridine ring in this determination are analogous to those in the enzyme active site further indicates that this orientation is critical for effective inhibition. The orientation of the benzoylglutamate moiety relative to the pteridine ring is more flexible and can readily accommodate itself to the enzyme requirements. Therefore, several low-energy conformations of MTX are accessible.

In summary, the results of this analysis show that (a) the molecular conformation of MTX is different from that observed in the two bacterial DHFR structures, (b) the intermolecular N···O contacts in the crystal structure are relevant to those found in the enzyme active site environment, and (c) MTX is protonated at N(1). These data also provide reliable details of the hydrogen bond strengths and directionality.

Acknowledgment. This research was supported in part by grants from NCI (CA34714) and FRA (287) (V.C.) from the American Cancer Society Faculty Research Award and the Buffalo Foundation. We acknowledge the assistance of Phyllis D. Strong, Dr. Patrick Van Roey, Dr. Walter Pangborn, Elaine De Jarnette, Gloria Del Bel, and Melda Tugac.

Electrochemical Reductive Activation of Mitomycin C

Paul A. Andrews,*[1] Su-shu Pan, and Nicholas R. Bachur

Contribution from the The New Frank Bressler Research Laboratories, University of Maryland Cancer Center, Baltimore, Maryland 21201. *Received September 20, 1985*

Abstract: We have used the electrochemical techniques of cyclic voltammetry and preparative flow cell electrolysis to study the role of one-electron vs. two-electron transfer in the reductive activation of mitomycin C (MC) and a primary mitosene metabolite, 1,2-*cis*-2,7-diamino-1-hydroxymitosene (**6**), to reactive intermediates in polar aprotic solvents. Cyclic voltammetry of MC in DMF (0.1 M TEAP) showed that MC undergoes two quasi-reversible electron-transfer processes at −0.937 and −1.410 V vs. Ag/AgCl, saturated KCl. A following chemical reaction appeared to occur after transfer of a second electron at −1.410 V as indicated by an anodic wave at −0.710 V and a cathodic wave at −0.800 V that appeared upon multicycle scanning. Flow cell reduction at −0.950 V vs. Ag/AgCl, 3 M NaCl over graphite, formed the radical anion of MC in DMF or Me_2SO as characterized by EPR (g = 2.0045). When the radical anion of MC in DMF was mixed with water, parent MC and at least eight other products were generated as detected by HPLC. The one-electron-reduction product profiles showed a pH dependence. Flow cell reduction of MC at −1.450 V formed the dianion of MC in DMF or Me_2SO, which generated only two products when mixed with water. These products have been identified by mass spectral and NMR analyses to be 10-decarbamoyl-2,7-diaminomitosene (**14**) and 2,7-diamino-2,3-dihydro-6-methyl-1*H*-pyrrolo[1,2-*a*]indole-5,8-dione (**22**). Generation of **22** was completely suppressed when the dianion was added to phosphate buffer. Flow cell reduction of **6** in DMF at −1.200 or −1.500 V generated the radical anion (g = 2.0045) or dianion, respectively. These species both gave 1,2-*cis*-2,7-diamino-2,3-dihydro-6,9-dimethyl-1-hydroxy-1*H*-pyrrolo[1,2-*a*]indole-5,8-dione (**27**) as the sole product when mixed with water. These data provide evidence that one-electron reduction is sufficient to activate MC and its primary metabolites to reactive intermediates. Furthermore, the results suggest that one-electron transfer is the dominant mode of bioreductive activation since the HPLC profile of the radical-anion-generated products of MC closely resembled the profile of metabolites generated from reduction with purified flavoenzymes.

Mitomycin C (MC; **1**) is a quinone-containing antitumor antibiotic that alkylates DNA, RNA, and protein;[2] cross-links complimentary DNA strands;[3-5] and cross-links DNA with protein.[3,5] The covalent attachment of MC to DNA is believed to

0002-7863/86/1508-4158$01.50/0